Efficiency of Histidine-Associating Compounds for Blocking the Alzheimer's Aβ Channel Activity and Cytotoxicity

Nelson Arispe,* Juan Carlos Diaz,* and Michael Flora†
*Department of Anatomy, Physiology and Genetics, and Institute for Molecular Medicine; and †Biomedical Institute, Uniformed Services University School of Medicine, Uniformed Services University of the Health Sciences, Bethesda, Maryland

ABSTRACT The opening of the Alzheimer's Aβ channel permits the flux of calcium into the cell, thus critically disturbing intracellular ion homeostasis. Peptide segments that include the characteristic histidine (His) diad, His^{13} and His^{14}, efficiently block the Aβ channel activity, blocking Aβ cytotoxicity. We hypothesize that the vicinal His-His peptides coordinate with the rings of His in the mouth of the pore, thus blocking the flow of calcium ions through the channel, with consequent blocking of Aβ cytotoxicity. To test this hypothesis, we studied Aβ ion channel activity and cytotoxicity after the addition of compounds that are known to have His association capacity, such as Ni^{2+}, imidazole, His, and a series of His-related compounds. All compounds were effective at blocking both Aβ channel and preventing Aβ cytotoxicity. The efficiency of protection of His-related compounds was correlated with the number of imidazole side chains in the blocker compounds. These data reinforce the premise that His residues within the Aβ channel sequence are in the pathway of ion flow. Additionally, the data confirm the contribution of the Aβ channel to the cytotoxicity of exogenous Aβ.

INTRODUCTION

A consensus on the primary mechanisms that cause neuronal damage in Alzheimer's disease (AD) remains elusive, but numerous reports have associated the cytotoxicity of amyloid beta peptides (Aβ) with the neurodegeneration observed in specific brain areas of AD patients (1–4). It has been shown that addition of fresh aggregates of Aβ to cell cultures generates a potentially toxic increase in the intracellular calcium concentration (5–9). Years of research supports the concept that disturbances of intracellular calcium homeostasis may play a pathological role in the neurodegeneration associated with AD (10–13).

A mechanism for the Aβ peptide-induced increase in intracellular calcium was originally proposed based on the formation of an independent tromethamine and aluminum-sensitive Aβ channel (14). This Aβ channel, which permits the entrance of extracellular calcium ions into the cell (15,16), has been confirmed in a variety of membranes by many researchers over the past decade (17–22), has been observed with atomic force microscopy (AFM) (23,24), and has been subjected to theoretical modeling (25–27). The asymmetry in one of the models (25) explains our finding that zinc preferentially binds and blocks only one side of the Aβ channel (28). It has been frequently demonstrated in studies of different metalloproteases, as well as in the Aβ molecule, that sites rich in histidine (His) and anionic residues are associated with Zn^{2+} binding (29–33). Because of the unique chemical nature of the His residue, it has a strong metal affinity. His residues act as a ligand to a metal center (34) bridging imidazole groups from the side chains of His residues (33). In the theoretical models of Durell et al. (25), the least energy calculations for the full size Aβ channels, imbedded in a lipid environment, position the rings of His^{13} and His^{14} of the Aβ molecule around the entrance of the putative pore. To test this prediction for the modeling algorithm, we recently showed that peptide segments that copy sectors of the sequence of the Aβ molecule containing the two neighboring His^{13} and His^{14} residues effectively block Aβ channel activity in planar lipid bilayers (16,35,36). When the His-His diad is substituted with residues that lack a propensity to interact with His residues, the peptides lose their effectiveness to both block the Aβ channel and prevent Aβ peptide cytotoxicity (36). Furthermore, methylation of the imidazole side chains of His residues in the Aβ peptide prevents the formation of His bridges, and also results in abolition of Aβ peptide neurotoxicity (37). We have interpreted these data to indicate that the blocker peptides containing the His-His diad form conventional coordination complexes with complementary His-His diads in the other Aβ subunits of the Aβ channel. Disruption of these complexes by the His-His diadic peptide segments prevents the formation of the potentially toxic Aβ channels. Therefore, we now hypothesize that compounds that are known to have His coordinating capacity, such as Ni^{2+}, imidazole, His, and His-related compounds should interfere with the currents and cytotoxicity of Aβ channels. We report here that the hypothesis is supported by the experimental data. We found that His-coordinating and His-related compounds can efficiently block Aβ channels incorporated in artificial membranes, and can also entirely prevent Aβ cytotoxicity. Therefore, we believe that these results reinforce the concept that the toxicity of the Aβ peptide on cells is basically exerted through the

Submitted April 17, 2008, and accepted for publication August 15, 2008.

Address reprint requests to Dr. Nelson Arispe, Dept. of Anatomy, Physiology and Genetics. School of Medicine, Uniformed Services University of the Health Sciences, 4301 Jones Bridge Rd., Bethesda, MD 20814. Tel.: 301-295 9367; Fax: 301-295 1715; E-mail: narispe@usuhs.mil.

Editor: Toshinori Hoshi.

0006-3495/08/11/4879/11 $2.00

doi: 10.1529/biophysj.108.135517

capacity of Aβ peptide to form Aβ ion channels in the cell surface membrane.

MATERIALS AND METHODS

Planar lipid bilayer methodology

A suspension of palmitoyloleoyl phosphatidylserine and palmitoyloleoyl phosphatidylethanolamine (Avanti, Alabaster, AL), 1:1, in *n*-decane was prepared. This suspension was applied to an orifice of ~100–120 μm diameter with a Teflon film separating two compartments, 1.2 mL volume each. The ionic solutions in the compartments contained asymmetrical concentrations of CsCl (200 cis/50 trans mM) and symmetrical 0.5 mM $CaCl_2$ and 5 mM K-HEPES, pH 7. The two ionic compartments were electrically connected to the input of a voltage clamp amplifier. Current was recorded using a patch clamp amplifier and data were stored on computer disk memory. Offline analysis of the channel activity was carried out using the software package pClamp (Axon Instruments, Foster City, CA). Incorporation of Aβ peptide into the bilayer was obtained by adding an aliquot of proteoliposome (Aβ-liposome) suspension to the solution in the *cis* side of the planar lipid bilayer chamber and stirring.

Preparation of proteoliposomes

Liposomes were prepared by hydration of air-dried palmitoyloleoyl phosphatidylserine (10 mg) with 1 M potassium aspartate, pH 7.0 (1 mL), followed by water sonication for 5 min. The liposome suspension (50 μL) was mixed with a stock aqueous solution of Aβ peptide (1 mg/mL, obtained from Bachem, Torrance, CA, and AnaSpec, San Jose, CA), followed by sonication.

Materials and His-related compounds

$NiCl_2$, imidazole, and L-His were purchased from Sigma-Aldrich (St. Louis, MO). The His-related compounds NAHIS01 (Ac–His–CONH2), NAHIS02 (Ac–His–His–CONH2), and NAHIS04 (Ac–His–His–His–His–CONH2), which contains one, two, and four His residues, respectively, were synthesized as amide and capped in the amino terminal with acetic anhydride. NAHIS02-(π-Met) (Ac–His-π-Met–His-π-Met–CONH2) was synthesized combining Fmoc-His(3-Me)-OH (Fmoc-His(π-Me)-OH; Bachem), which possesses the imidazole group methylated at the π position.

Cell culture

PC12 cells, derived from a transplantable rat pheochromocytoma (ATCC No. CRL 1721), were cultured in the recommended ATCC medium. Primary cultures of hippocampal and cortical neurons from P18-P21 rat brains were grown in neurobasal medium/B27 (GIBCO, Carlsbad, CA). For neuron preparation, pregnant rats were anesthetized and killed to extract the fetuses. For pain alleviation, the animals were anesthetized following recommendations in the 2000 Report of the American Veterinary Medical Association Panel on Euthanasia. Brains from the fetuses were dissected out and neuronal cell cultures were prepared as in a previously described protocol (9).

Cell viability assays

The percentage of cells protected from Aβ-induced cell death by various treatments was evaluated by means of a colorimetric XTT assay (Cell Proliferation Kit II, Roche, Mannheim, Germany). The cytotoxicity was also directly measured by the release of lactate dehydrogenase (LDH) from the cytosol into the media (Cytotoxicity Detection Kit (LDH), Roche).

RESULTS

Effect of Ni^{2+} and imidazole on the Aβ ion channel electrical activity

Based on the theoretical model proposed by Durell et al. (25), the predicted pore region of the Aβ channel is made of the hydrophilic structure composed of residues 1–16. The structure formed by a radial polymer of four to six Aβ subunits predicts that rings of His residues surround and form the path for the ions passing through the pore. The results from our previous work (36,37) show that the common feature of the active Aβ channel blocker peptides is that they all possess in their sequence the two vicinal His residues that have been modeled as lining the entry to the pore. It is therefore possible that compounds of known His coordinating capacity will interact with His in the mouth of the pore. This interaction will block the entrance to the Aβ pore, and consequently affect the flow of current through the Aβ channel. We studied various compounds of known His coordinating capacity for their interaction with Aβ channels incorporated into planar lipid bilayers. No membrane potential difference was applied to the lipid bilayers, to avoid any disturbing effect the membrane potential might have on the channel activity and the conformations of the channel. The experiments depicted in Fig. 1 *A* show that when incorporated into a lipid bilayer, the Aβ channel operates between multiple conductance levels. One channel is responsible for the multiple conductance levels and each channel incorporation may show a different pattern of conductance transitions, as has been described elsewhere (14,35). The insert in Fig. 1 *A* shows that discrete jumps of current to different levels (1.46, 2.92, 5.03, and 10.17 pA) can be observed throughout. The addition of Ni^{2+}, which coordinates with imidazole with high affinity, and imidazole, which has a preference to have an interplanar interaction with other aromatic residues, blocks the current activity of Aβ channels incorporated in lipid bilayers. After the ionic current through the incorporated Aβ channels appeared stable for several minutes, either Ni^{2+} or imidazole was added to the experimental chamber. The current records in the figure display 8 s of activity from the Aβ channels, maintained at zero membrane potential, before (control) and several seconds after the channels were exposed to either Ni^{2+} (Fig. 1 *A*) or imidazole (Fig. 1 *C*). The channel activity slowly reduced to an undetectable level, suggesting a full block of the channel. The blockage by both Ni^{2+} (not shown) and imidazole (bottom record of Fig. 1 *C*) was irreversible since the channels remained fully blocked after the chamber was washed. Amplitude histograms of the current events during same time intervals of channel activity before and at different times after the addition of the test compounds were elaborated and are displayed in the right panels of Fig. 1, *B* and *D*. The histograms show that both Ni^{2+} and imidazole are effective at quickly abolishing the number of observations of the most frequent peak current values (0.8, 3.2, 5.2, 7.5, and 10 pA).

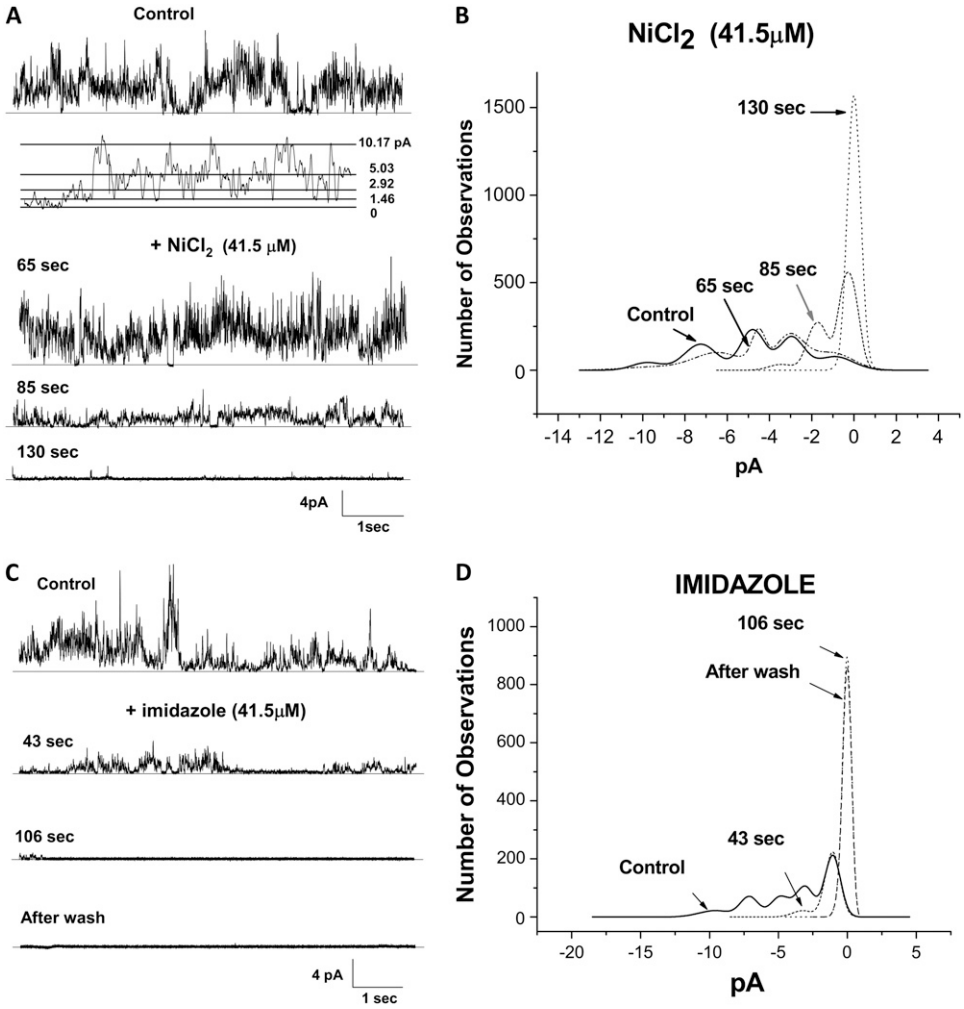

FIGURE 1 Nickel and imidazole irreversibly block the membrane-bound Aβ ion channel. (*A* and *C*) Electrical activity across a lipid bilayer with incorporated Aβ channels, recorded before (control) and in the presence of either Ni^{2+} (*A*) or imidazole (*C*). The membrane electrical potential in the experiment was maintained at zero level. *B* and *D* display the current amplitude histograms of the channel activity from the current traces in *A* and *C*. Five main current peaks of 0.8, 3.2, 5.2, 7.5, and 10 pA characterize the Aβ channel activity. Both compounds quickly abolish the most frequent current peaks.

Effect of His on the Aβ ion channel electrical activity

We have previously shown that His residues are essential components in the sequence of active Aβ ion channel blocker peptides (36,37). His is an aromatic amino acid that contains a heteroaromatic imidazole ring available for interaction. To study the contribution of the imidazole ring in the His interaction with the Aβ ion channel, we investigated the channel blocking efficiency of a modified, end-capped His (NAHIS01) and compared it with the blocking efficiency of the unmodified, amino and carboxyl ends-free His. The end-capped His, with the carboxyl and amine group amidated and acetylated, respectively, would leave the imidazole side chain as the sole group available for interaction with other reactive groups in the Aβ channel.

The current activity from Aβ channels illustrated in Fig. 2 indicates that both unmodified His and modified His NAHIS01 affect the peaks of ionic current from an Aβ channel incorporated in a lipid bilayer. The current records in Fig. 2, *A* and *C*, and the current amplitude histograms in the Fig. 2, *B* and *D*, show that unmodified His mildly reduces the Aβ channel activity and is relatively ineffective at producing an irreversible full block of the Aβ channels. The peaks of ionic current corresponding to larger channel conductance (5.8 and 4.2 pA) are blocked in a concentration-dependent manner, but the smaller current peaks remain unaffected at the highest concentration of His. As shown in Fig. 2, *C* and *D*, although the modified His NAHIS01 failed as a full channel blocker, it more effectively reduced the Aβ channel activity at lower concentrations.

The Aβ channel blocking efficiency of His-related compounds increases with the number of imidazole side chains

In the previous experiments we showed that NAHIS01, in which the imidazole is the sole group available for interaction, is very efficient at blocking the Aβ ion channel. Here we studied the ability of two His-related compounds, NAHIS02 and NAHIS04, to block Aβ channels. These compounds possess two and four imidazole side chains, respectively. The current records and current amplitude histograms from Aβ

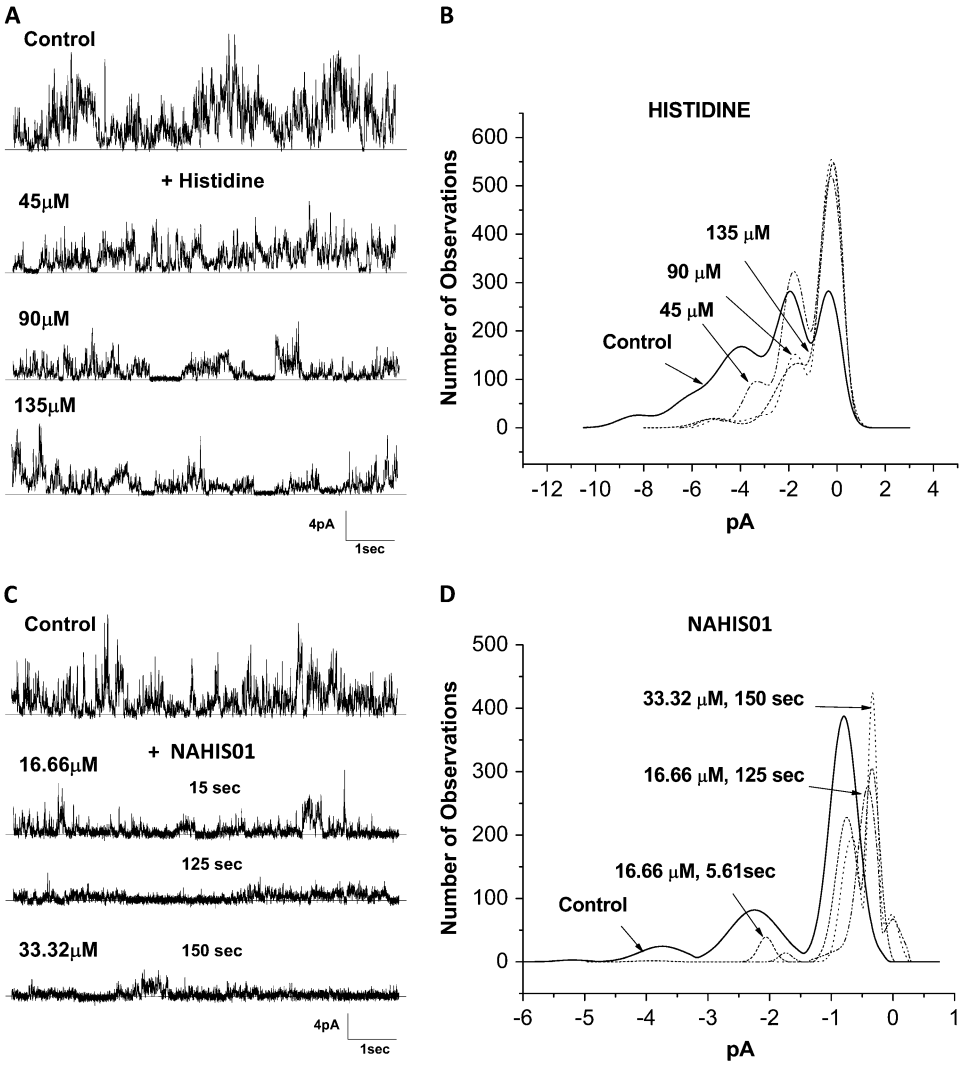

FIGURE 2 Efficacy of His to block the Aβ channel is improved by capping its amino and carboxyl ends. (*A* and *C*) Electrical activity from two lipid bilayers with incorporated Aβ channels, recorded before (control) and while the Aβ channel was exposed to various concentrations of unmodified, amino and carboxyl ends-free His, and a modified His, NAHIS01, with the carboxyl and amine groups amidated and acetylated. The Aβ channels were exposed to each concentration of the blocker compounds for 2-min periods. Increases in the concentration of the unmodified His only affect the current peaks of 5.8 and 4.2 pA, corresponding to larger channel conductance. NAHIS01 is more effective at reducing all current peaks at much lower concentrations than unmodified His. *B* and *D* display the amplitude distribution histograms of the ionic current peaks recorded while the Aβ channel was exposed to each concentration of His and NAHIS01, respectively.

channels, before and after exposure to the two His-related compounds, are illustrated in Fig. 3. During the current recording the bilayer was maintained at zero membrane potential. The current records in Fig. 3, *A* and *C*, show that both compounds efficiently block the multiple conductances exhibited by the Aβ channels. However, one of the distinguished observations is an apparent higher affinity by NAHIS04 for the channel that stayed fully blocked after the chamber was washed. The lower current record in Fig. 3 *C* shows that NAHIS04, which possesses four imidazole side chains, is the most effective at irreversibly blocking the Aβ channel activity. The lower current record in Fig. 3 *A* shows some recovery of channel activity after NAHIS02 was washed off. No effect of membrane potential in the blocking capacity of these compounds was observed (not shown). We previously reported that the level of the membrane potential has no effect on the ability of similar His-related compounds to block the Aβ channel (35). The current amplitude histograms in Fig. 3, *B* and *D*, show a gradual reduction in the number of current peaks after the Aβ channels are exposed to either one of these His-related compounds. The results reveal that the number of imidazole side chains in the blocker compounds has a substantial influence on their efficiency for blocking the Aβ channel conductance. The experiment illustrated in Fig. 3 *C* shows that NAHIS04 (16.66 μM), which possesses four imidazole side chains, reduced the Aβ channel activity to occasional channel openings just 20 s after addition. By contrast, at the same concentration, NAHIS02, which possesses two imidazole groups, takes several minutes to produce similar levels of channel blockage.

The contribution of the imidazole side chains in the His-related compounds to block the Aβ channel activity was verified with the experiments shown in Fig. 4. Here the effectiveness of the His-coordinating and His-related compounds was studied in terms of the time required to block the Aβ channel currents. The top current record in Fig. 4 *A* displays the time course of the Aβ channel activity before and after the addition of the channel blocker NAHIS02. The bottom current record displays the channel activity from a similar experiment in which increasing concentrations of

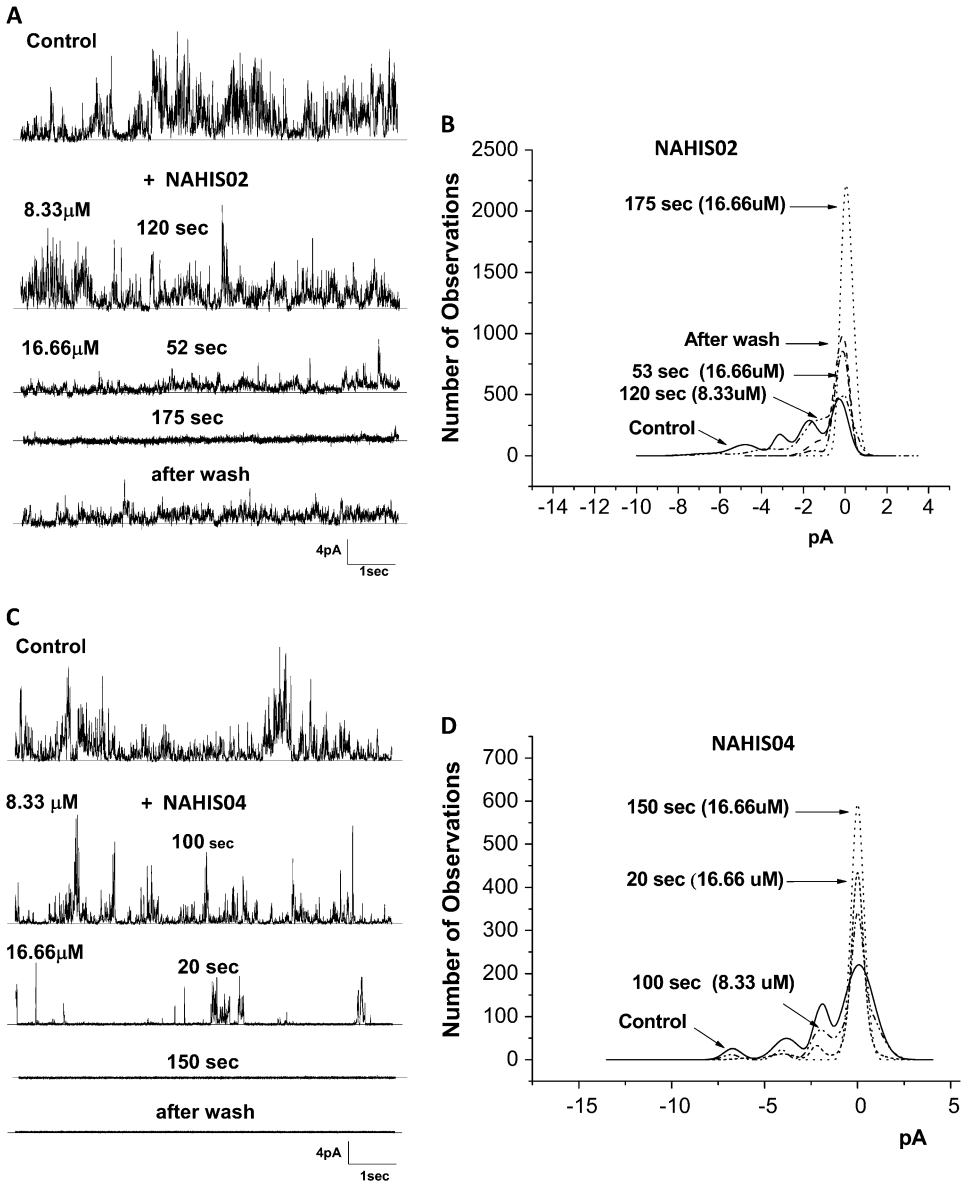

FIGURE 3 Aβ channel blocking efficiency of His-related compounds increases with the number of imidazole side chains. (*A* and *C*) Electrical activity from two lipid bilayers with incorporated Aβ channels, recorded before (control) and while the Aβ channels were exposed to two compounds that possess two (NAHIS02) and four (NAHIS04) imidazole side chains, respectively. The current records show the channel activity at various times after the channels were exposed to two concentrations of the blocker compounds. After full blockage of the Aβ channel, the blocking action of NAHIS02 reversed when the experimental chamber was washed of the blocker. The blockage by NAHIS04 was irreversible. *B* and *D* display the amplitude distribution histograms of the ionic current peaks recorded while the Aβ channel was exposed to various concentrations of NAHIS02 and NAHIS04, respectively. At a concentration of 16.66 μM both compounds removed all current peaks. However, NAHIS04 produced full blockage more quickly.

a modified NAHIS02, NAHIS02-(π-Met), were added. NAHIS02-(π-Met) is a modified NAHIS02 in which the imidazole side chains are methylated. The unmodified NAHIS02, at 16.66 μM, totally blocks the Aβ channel activity in <3 min. In contrast, NAHIS02-(π-Met) is unable to block the Aβ channel activity even at a fourfold higher concentration, indicating that the methylation of the imidazole groups reduces the affinity of NAHIS02 for the Aβ molecule and consequently the ability to block the Aβ channel. When Aβ channels are incorporated into artificial membranes, they form multiconductance systems. This is manifested by frequently fluctuating conductance between specific levels. To comparatively evaluate the blocking strength of the test compounds in terms of the time required to stop the Aβ channel activity, experiments similar to that displayed in Fig. 4 *A* were performed with each one of the test compounds. The results were analyzed by an alternative procedure that quantifies the total ionic current flowing through the Aβ channel incorporated into the artificial lipid membrane at any given time. For this purpose, we integrated the total ionic current flowing through the membrane and averaged the amount of charge conducted in consecutive time intervals of 8 ms duration. The integration was initiated after the incorporated channel achieved stable activity, and also after the addition of the test compounds. The left panel plot in Fig. 4 *B* shows that imidazole is extremely efficient at promptly (30 s) blocking the flow of ionic charges, in contrast to His, which was very slow-acting or had almost no channel-blocking capacity. Ni^{2+} ions, as also shown in Fig. 2 *A*, fully blocked the Aβ channel within a few seconds (120 s). The plot in the right panel in Fig. 4 *B* shows that the efficiency for stopping the Aβ channel activity of the His-related compounds ap-

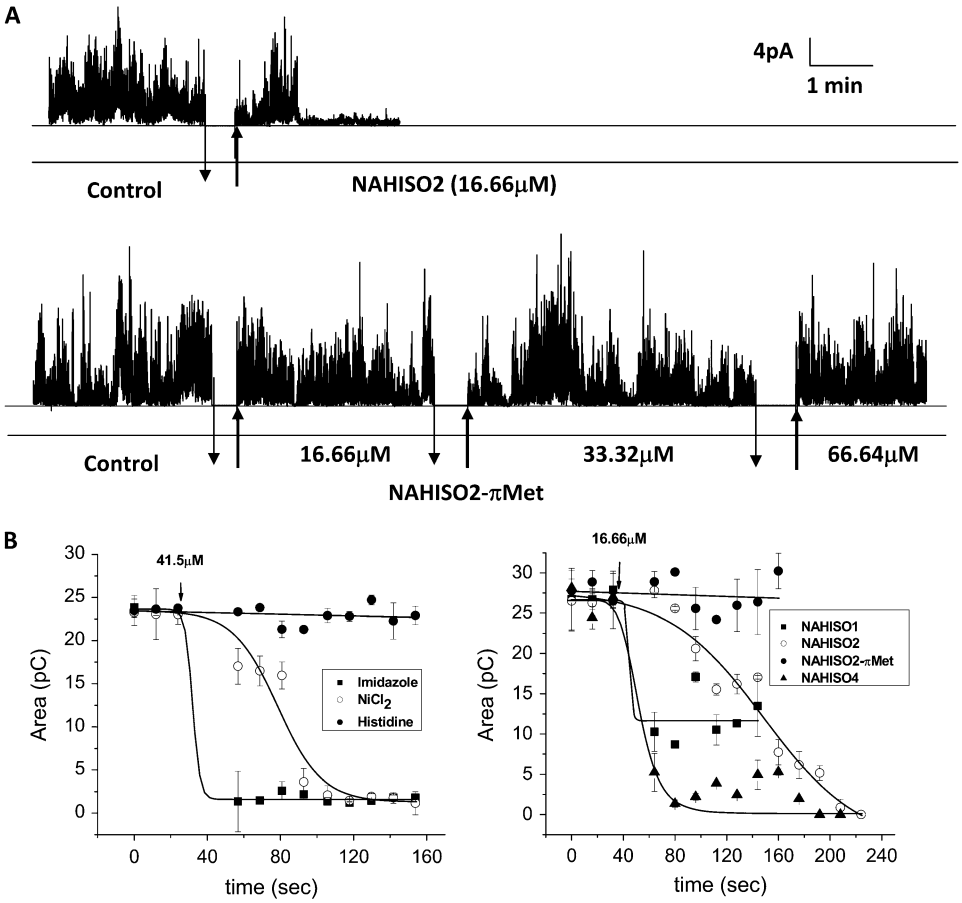

FIGURE 4 Time course of ionic charge conducted by membrane-incorporated Aβ channels, showing the effect of Aβ channel blockers. (*A*) The current records show the time course of the activity of Aβ channels incorporated into planar lipid bilayers before and after the addition of the Aβ channel blocker NAHIS02 (*top record*) and NAHIS02-(π-Met) (*bottom record*). The concentration of NAHIS02-(π-Met) was gradually increased as indicated, at the times signaled by the arrows. NAHIS02-(π-Met) did not affect the Aβ channel activity even at a fourfold higher concentration. (*B*) The amount of charge conducted by bilayer-incorporated Aβ channels before and after the addition of imidazole, Ni^{2+}, and His at concentrations of 41.5 μM (left plot), and NAHIS01, NAHIS02, NAHIS02-(π-Met), and NAHIS04 at a concentration of 16.6 μM (right plot). The ionic current flowing through the membrane was integrated in consecutive time intervals of 8-ms duration. The efficiency to stop Aβ channel activity increases as the number of imidazole side chains in the blocker compounds is increased. pC: picoCoulombs.

pears to increase as the number of imidazole side chains in the His-related compound is increased. Hence NAHIS04, which has four imidazole side chains, reduces the flow of ionic charges through the membrane by 50% in 15 s. This reducing effect is eightfold faster compared to the 125 s it takes for NAHIS02, which has two imidazole side chains, to achieve the same level of reduction. In contrast, NAHIS01, which only has one imidazole side chain, does not fully prevent the flow of ionic charges, and NAHIS02-(π-Met), from which imidazole reactivity is removed by methylation, showed no blocking capacity.

Protection of cells from the Aβ cytotoxicity increases in efficiency with the number of imidazole groups in the Aβ channel blocker

We have previously shown that Aβ cytotoxicity can be prevented when cells are incubated in media containing Aβ channel blockers (9,16,37). Since Ni^{2+}, imidazole, His, and His-related compounds affect, to different degrees, Aβ channels incorporated into artificial membranes, we examined the ability and relative strength of these compounds to protect cells from Aβ peptide-induced cell death. Cell viability was examined using two different assays. These were the colorimetric XTT assay that quantifies metabolically active cells, and an assay that measures the release of LDH from the cytosol into the media, which evaluates the cell membrane integrity. The panels in Fig. 5 show the viability of PC12 cells (*A* and *B*), and cortical (*C* and *D*) and hippocampal neurons (*E* and *F*) observed after 3 days of incubation in the presence of Aβ peptide (5 μM) and Aβ peptide (5 μM) plus Ni^{2+}, imidazole, or His. The left panels (*A*, *C*, and *E*) show the results from the XTT assay expressed as a percentage of cytotoxicity, and the right panels (*B*, *D*, and *F*) show the results from the measurements of LDH released from cells into the media expressed as a percentage of protection of cells. The performance of imidazole, Ni^{2+}, and His to maintain cell viability and protect cells from Aβ peptide-induced cell death strongly corresponds to what one would expect from their effects displayed on the ionic current flowing through the Aβ channels incorporated into artificial membranes. Imidazole and Ni^{2+} were found to fully protect the cells against Aβ cytotoxicity, but Ni^{2+} showed a cell-dependent toxicity at high concentrations. On the other hand, His, which mildly reduced the Aβ channel activity, performed poorly in protecting cells from Aβ toxicity. The panels in Fig. 6 show the viability of PC12 cells (*A* and *B*), and cortical (*C* and *D*) and hippocampal neurons (*E* and *F*) observed after 3 days of incubation in the presence of Aβ peptide (5 μM) and Aβ peptide (5 μM) plus the His-related

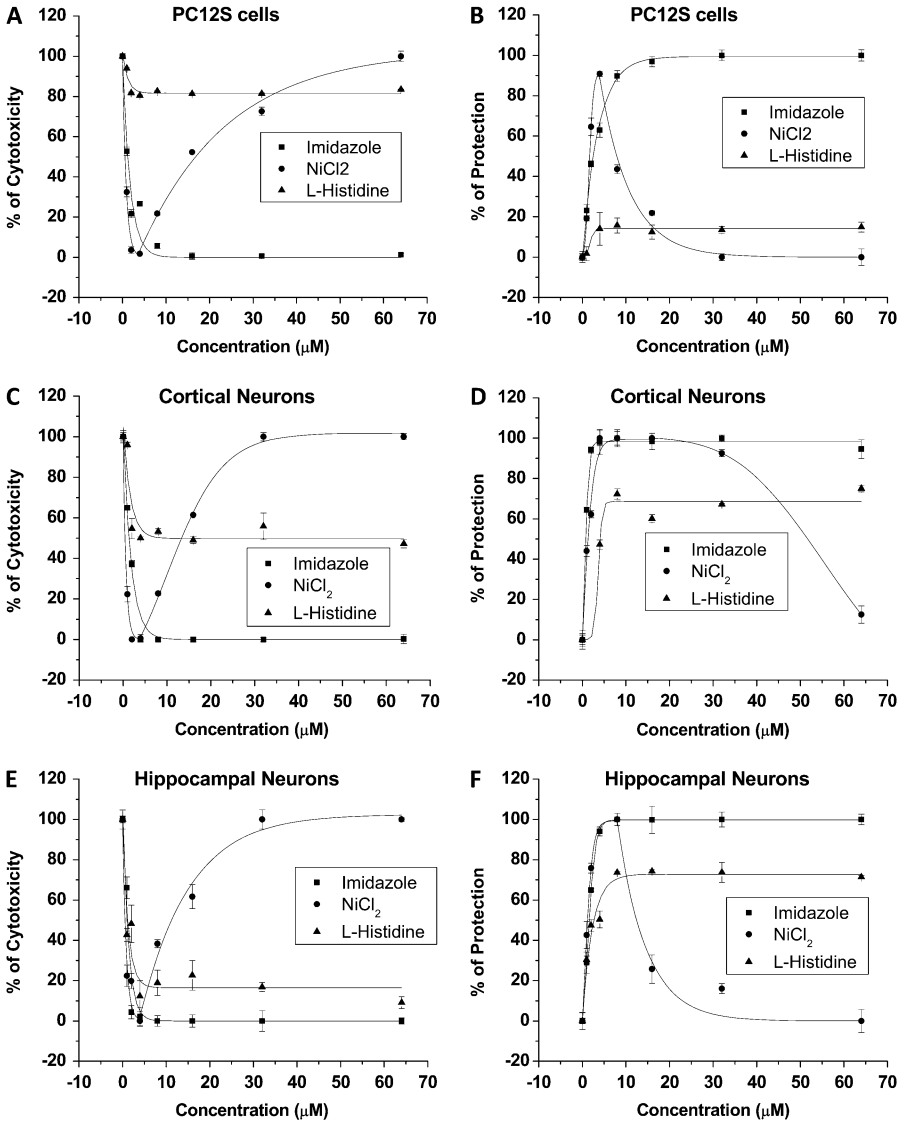

FIGURE 5 Protection of cells from Aβ cytotoxicity by compounds that coordinate and associate with Aβ channels. Viability of PC12S cells (*A* and *B*), and cortical (*C* and *D*) and hippocampal neurons (*E* and *F*) observed after 3 days of incubation in the presence of Aβ peptide (5 μM) and Aβ peptide (5 μM) plus Ni^{2+}, imidazole, or His. The results from the XTT assay are expressed as a percentage of cytotoxicity (*A*, *C*, and *E*). The LDH released from cells into the media is expressed as a percentage of protection of cells (*B*, *D*, and *F*). Imidazole and Ni^{2+} fully protect cells against Aβ cytotoxicity, but Ni^{2+} showed a cell-dependent toxicity at high concentrations. His performed poorly in protecting cells from Aβ toxicity.

compounds NAHIS01, NAHIS02, NAHIS02-(π-Met), or NAHIS04. The left panels (*A*, *C*, and *E*) show the results from the XTT assay as a percentage of cytotoxicity, and the right panels (*B*, *D*, and *F*) show the results from the measurements of LDH release into the media as a percentage of protection of cells. The performance of the His-related compounds to protect cells from the Aβ peptide-induced cell death also strongly corresponded to what one would expect from their effects displayed on the ionic current flowing through the Aβ channels incorporated into artificial membranes. NAHIS02 and NAHIS04 fully protected the three different types of cells against Aβ. NAHIS01, which did not fully block Aβ channels in artificial membranes (see Fig. 3), showed partial protection. The level of protection for all these compounds correlated with the number of imidazole side chains in these compounds. For instance, the concentration required for 50% protection (half maximal effective concentration, EC_{50}) for the three different types of cells for the compounds NAHIS02 and NAHIS04 was always below 1 μM. The EC_{50} for imidazole was between 2 and 3 μM (see Fig. 6). The compound NAHIS02-(π-Met) was very inefficient at protecting against Aβ peptide cytotoxicity. The mild protection observed with this compound was cell-type dependent and always plateaued at much higher concentrations than that observed with the unmethylated form. Full methylation of NAHIS02-(π-Met) is never achieved during the synthesis process. Therefore, a mild protection is not totally unexpected to be observed in the results. However, the loss of protection strongly suggests that the methylation of NAHIS02 is affecting at the site of the molecule that interacts with the Aβ channel.

DISCUSSION

The results described in this investigation show that His-coordinating and His-related compounds can efficiently block Aβ channels incorporated into artificial membranes,

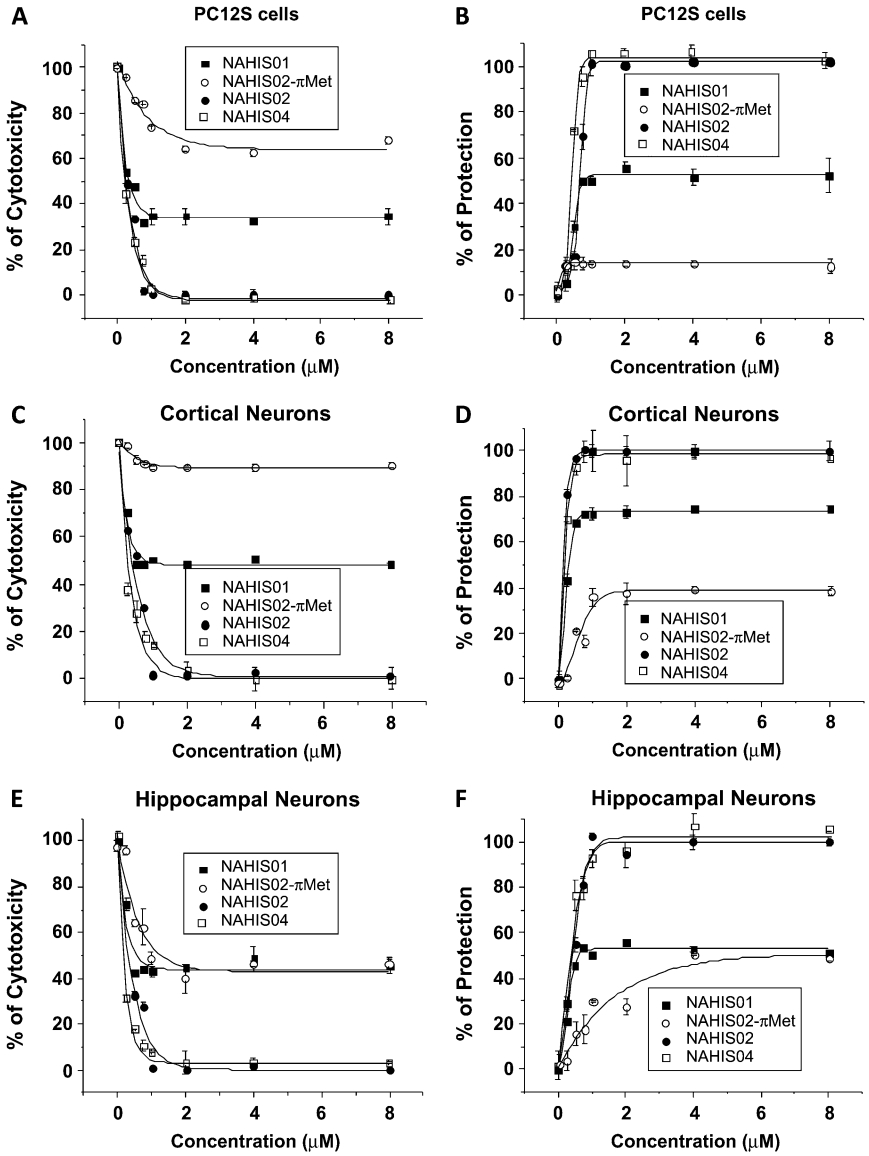

FIGURE 6 Protection of cells from Aβ cytotoxicity by His-related compounds that establish aromatic interaction with Aβ channels. Viability of PC12 cells (*A* and *B*), and cortical (*C* and *D*) and hippocampal neurons (*E* and *F*) observed after 3 days of incubation in the presence of Aβ peptide (5 μM) and Aβ peptide (5 μM) plus NAHIS01, NAHIS02, NAHIS02-(π-Met), and NAHIS04. The results from the XTT assay are expressed as a percentage of cytotoxicity (*A*, *C*, and E). The LDH released from cells into the media is expressed as a percentage of protection of cells (*B*, *D*, and *F*). The level of protection for all these compounds correlated to the number of reactive imidazole side chains. NAHIS02 and NAHIS04 fully protected the cells against Aβ. NAHIS02-(π-Met) was very inefficient at protecting against Aβ peptide cytotoxicity.

and can also entirely prevent Aβ cytotoxicity produced by the incorporation of Aβ channels in the cell surface membrane. Therefore, we interpret these data to support the hypothesis that His residues within the Aβ channel sequence are in the pathway of ion flow and contribute to define the ion channel selectivity. Additionally, the data confirm the contribution of the Aβ channel to the cytotoxicity of Aβ.

We previously reported that small peptides designed to closely match the sequence of the Aβ peptide that includes His^{13} and His^{14} were the most effective at blocking ion currents through Aβ channels (35,36). The results of the investigation presented here strongly suggest that Aβ channel blockage by compounds of known His-coordinating capacity, such as Ni^{2+} and imidazole, occurs by the interaction with the His residues located in the pathway of the ions in the Aβ channel. This conclusion is supported by the enhanced blocking efficiency observed after increasing the number of imidazole reactive side chains in His-related compounds. Additionally, we observed that perturbing the bonding of the imidazole side chains by selective methylation, which prevents the interplanar interaction of imidazole with the aromatic His residues, results in abolition of Aβ channel current activity and neurotoxicity.

Binding sites for the Aβ channel blockers

The highly effective block of the Aβ channels observed in our experiments after the application of either nickel (Ni^{2+}) or imidazole is expected if the His in the Aβ subunits of the Aβ channels are the participating residues. Information collected from the Protein Data Bank reveals that among the aromatic residues His can be found in various chemical environments

in protein structures, sometimes behaving as an aromatic residue, or as a metal ligand, and at other times forming salt bridges with acidic groups (38). The interaction between His and Ni^{2+} is so profound that the His tag is globally the most used tag in the preparative purification of proteins. Immobilized metal affinity chromatography, which is used to purify His-tagged proteins, exploits the ability of His to bind chelated transition metal ions, and Ni^{2+} has generally been proven to be the most successful of the metal ions. Competitive interaction is the most common method used to recover the purified protein fractions. Imidazole competitively interacts with immobilized Ni^{2+} ions to reverse the binding of the protein. With the exception of nickel, the compounds that we found in this investigation to be efficient for blocking the Aβ channels were aromatic residues containing the heteroaromatic imidazole ring. As a heteroaromatic moiety, imidazole can interact with other aromatic and nonpolar groups, since it can exist in the neutral or positively charged form at the physiological pH. Additionally, imidazole can form the most conspicuous hydrogen bonds with polar and charged (both negative and positive) residues (39,40). Depending on the protonation state, imidazole can also be involved in salt bridges with acidic groups. For these reasons, it is expected that effective interactions can be established between the imidazole-containing compounds that block Aβ channels and the charged His^6, His^{13}, His^{14}, Glu^{22}, and Lys^{28} residues in the Aβ subunits in the Aβ channel. However, among the charged residues in the Aβ subunit sequence, His is the only aromatic residue and is the most likely candidate to carry the preferred face-to-face geometric interactions with imidazole (38). Imidazole is a five-membered planar ring that consists of one π electron from the =N-atom, one from each carbon atom, and two from the NH nitrogen. This resonance structure makes imidazole an excellent nucleofile that would be attracted to a full or partial positively charged form of the His in the Aβ subunits of the Aβ channels. Therefore, the propensities of imidazole to interact with His residues vastly overcome the propensities to interact with the other charged residues, such as Lys or Glu, in the Aβ subunit (38,40,41). In the case of the His-related compounds tested for blocking the Aβ channel, we observed a remarkable increase in blocking efficiency because the blocker compounds possess more available reactive imidazole side chains. In contrast, NAHIS02, which behaved as a highly efficient blocker, not only lost its capacity to block the Aβ channels, but additionally became ineffective in protecting from Aβ cytotoxicity when the imidazole side chains were perturbed by methylation. A large number of studies have dealt with the subject of aromatic–aromatic interaction in proteins. The vast majority of medicinal agents contain aromatic substituents and their differential recognition by proteins is likely to be facilitated by the noncovalent interactions involving aromatic residues (42). Among the aromatic residues, His has the highest propensity to interact with planar groups and forms a distinct class separate from all other residue types (40,41).

The function of the imidazole side chain in the His interaction with the Aβ ion channel

We observed that the efficacy for blocking the Aβ channel by the amino acid His is improved when the free ends of His are modified by amidation and acetylation of the carboxyl and amine groups, respectively. This modification, in addition to making the peptide resistant to proteases degradation, reduces the peptide unspecific reactivity. Our interpretation of the improved blocking efficacy of NAHIS01 compared to the ends-free His is that in the unmodified His, in addition to the imidazole side chain, the free ends increase the possibility for His to unspecifically interact with any other reactive residues present in the Aβ subunits of the Aβ channel. Therefore, the unspecific interactions with other regions of Aβ reduce the probability of specific interactions with His that form the ion-conducting path of the Aβ channel. When the His ends are capped and are unable to chemically react, as is the case with NAHIS01, the reactivity of His is restricted to the specific interaction that may be established by its imidazole side chain. Thus, the probability for aromatic interactions between the exceptionally nucleofilic imidazole in the ends-capped His and the imidazole side chain in the participating His in the Aβ channel will be increased. We believe that the improved efficacy of the ends-capped NAHIS01 compared to ends-free His, as an Aβ channel blocker, is further proof of the concept that the aromatic interaction between the imidazole side chains contributes to the blocking of Aβ channels.

Blocking of Aβ channels preserves cells from Aβ cytotoxicity

The efficacy of His coordinating compounds for preserving cells from Aβ cytotoxicity was tested in three different types of cells. Initially, the preservation of the viability of cells observed in cases where specific Aβ channel blockers were used in combination with Aβ confirmed the participation of the Aβ channels in Aβ cytotoxicity (9,36). Those compounds that were observed to fully block Aβ channels incorporated into artificial membranes were also found to be efficient at preserving cell viability during exposure to the toxic Aβ peptide. The results were obtained from three different cell types by the application of two different viability assays. It has been shown that the interaction between Aβ peptides and the cell surface membrane is followed by activation of an intracellular signaling cascade that leads to the death of cells by apoptosis (43). The finding that Aβ channel blockers fully prevent cell death corroborates the formation of Aβ ion channels as the initial step in the changes associated with the Aβ-induced apoptosis (9), and suggests that channel formation is the main mechanism by which Aβ exerts its toxicity. Additionally, the data shown here confirm that exposure of cells to Aβ results in the formation of oligomeric Aβ aggregates, which assemble the Aβ channels as they interact with the cell surface membrane. This is the first step in the

signaling cascade that leads to cell death. The results from the application of viability assays on the three different types of cells show that the efficacy of the His-related compounds to preserve cells from Aβ cytotoxicity is correlated to the intensity of the interactions with the His residues in the Aβ channel. By increasing the number of reactive imidazole side chains in the blocker compound, the capacity to block the active Aβ channels incorporated into the membranes of the cells is also increased. Our results in cultured cells showed that the blocking efficacy of His-related Aβ channel blockers was improved to EC_{50} values below the micromolar levels, as was the case for the blockers NAHIS02 and NAHIS04. This represents a considerable improvement compared to the blocking effect obtained with previously published Aβ channel blockers (16,35,36).

Our experimental results and the theoretical models of the Aβ channel

The channel-like annular structure of Aβ oligomers, as has been observed by electron microscopy (44) and by AFM (23,24), suggests that to form an Aβ channel, Aβ subunits assemble in a polymeric transmembrane structure. Based on this structure, a series of theoretical models have been designed to shape the different forms that oligomers of Aβ assemble to form ion channels when incorporated into a lipid membrane (25–27). The most recently developed models, which illustrate the atomistic structure of the Aβ channel in annular topology, follow molecular-dynamics simulations based on nuclear magnetic resonance data of the oligomers and use the universal U-shaped (strand-turn-strand) motif for the truncated $A\beta^{17-42}$ (26,27). Although these models do not include the first 16 residues of the Aβ subunits, which contain the His residues, the negatively charged side chains of Glu^{22} are arranged circularly in the pore, inducing a cationic ring by the binding of cations such as Mg^{2+}, Ca^{2+}, K^{+}, and Zn^{2+} (26,27). Former models were developed based on least-energy calculations, and assume that the channels are formed from an assembly of Aβ subunits arranged symmetrically around the axis of a pore lined by an amphipathic array of alternated charged residues. In this case the resulting models present rings of His^{13} and His^{14} residues of the Aβ molecule around the entrance of the putative pore (25). If not all the His are protonated, this annular arrangement will model pores with a net negative charge to explain the cation selectivity of the Aβ channels. The theoretical models for the truncated $A\beta^{17-42}$ include the charged residues Glu^{22} and Lys^{28} of the Aβ subunit. The old model on energetic grounds for the full-length $A\beta^{1-40}$ includes in addition the charged residues His^{6}, His^{13}, and His^{14}. Although the molecular-dynamics simulations successfully reproduce the channel dimensions, shapes, and subunit organization of the Aβ channels observed with AFM (23,24), our results from using His-containing Aβ channel blockers could be better explained by a model that will represent the full-length Aβ subunit. Such a model must include His residues in addition to the Glu^{22} and Lys^{28} charged residues. There are examples of the amino end of the Lys side chain and Glu acid side chain interacting with His residues. However, His prefers to interact in a face-to-face stacked orientation with His rings (38,40). We speculate that this may provide stability to the assembly of Aβ subunits in a polymeric transmembrane channel structure. In this respect, disruption of this His-His interaction may prevent the functioning of Aβ channels. Recent experiments showed that perturbing the hydrogen bonding of the imidazole side chains of His residues of Aβ by selective methylation prevents the formation of His bridges and results in abolition of the Aβ neurotoxicity (37).

In conclusion, the addition of compounds of known His-coordinating capacity, such as Ni^{2+}, imidazole, His, and a series of His-related compounds, to Aβ channel incorporated in membranes show that the His residues located in the N-terminal branch of the Aβ peptide sequence are essential to form the functional structure that constitutes the selectivity filter and the ion pathway of the Aβ channel. To achieve the functional characteristic of the Aβ channels, the theoretical models, constructed to shape the different forms that oligomers of Aβ assemble to form ion channels, have to include the segment of the Aβ peptide that contains the charged His residues.

The authors thank Drs. Dave Mears and Richard Siarey for invaluable comments and critically reading the manuscript. This work was financially supported by the Alzheimer's Association of America and by grant CO70TS from the Uniformed Services University of the Health Sciences.

REFERENCES

1. Yankner, B. A. 1996. Mechanism of neuronal degeneration in Alzheimer's disease. *Neuron.* 16:921–932. (Review)
2. Yankner, B. A. 2000. The pathogenesis of Alzheimer's disease. Is amyloid β-protein the beginning or the end? *Ann. N. Y. Acad. Sci.* 924: 26–28.
3. Hardy, J. A., and G. A. Higgins. 1992. Alzheimer's disease: the amyloid cascade hypothesis. *Science.* 256:184–185.
4. Hardy, J. A., and D. J. Selkoe. 2002. The amyloid hypothesis of Alzheimer's disease: progress and problems on the road to therapeutics. *Science.* 297:353–356.
5. Mattson, M. P., B. Cheng, D. Davis, K. Bryant, I. Liberberg, and R. E. Rydel. 1992. β-Amyloid peptides destabilize calcium homeostasis and render human cortical neurons vulnerable to exicitoxicity. *J. Neurosci.* 12:376–389.
6. Kawahara, M., Y. Kuroda, N. Arispe, and E. Rojas. 2000. Alzheimer's β-amyloid, human islet amylin, and prion protein fragment evoke intracellular free calcium elevations by a common mechanism in a hypothalamic GnRH neuronal cell line. *J. Biol. Chem.* 275:14077–14083.
7. Zhu, Y. J., H. Lin, and R. Lal. 2000. Fresh and nonfibrillar amyloid β protein(1–40) induces rapid cellular degeneration in aged human fibroblasts: evidence for AβP-channel-mediated cellular toxicity. *FASEB J.* 14:1244–1254.
8. Demuro, A., E. Mina, R. Kayed, S. C. Milton, I. Parker, and C. G. Glabe. 2005. Calcium dysregulation and membrane disruption as a ubiquitous neurotoxic mechanism of soluble amyloid oligomers. *J. Membr. Biol.* 280:17294–17300.

9. Simakova, O., and N. Arispe. 2006. Early and late cytotoxic effects of external application of the Alzheimer's Aβ result from the initial formation and function of ion channels. *Biochemistry*. 45:5907–5915.
10. Mattson, M. P., S. W. Barger, B. Cheng, I. Lieberburg, V. L. Smith-Swintosky, and R. E. Rydel. 1993. β-amyloid precursor protein metabolites and loss of neuronal calcium homeostasis in Alzheimer's disease. *Trends Neurosci*. 16:409–415.
11. Kawahara, M. 2004. Disruption of calcium homeostasis in the pathogenesis of Alzheimer's disease and other conformational diseases. *Curr. Alzheimer Res*. 1:87–95.
12. LaFerla, F. M. 2002. Calcium dyshomeostasis and intracellular signaling in Alzheimer's disease. *Nat. Rev. Neurosci*. 3:862–872.
13. Smith, I. F., K. N. Green, and F. M. LaFerla. 2005. Calcium dysregulation in Alzheimer's disease: recent advances gained from genetically modified animals. *Cell Calcium*. 38:427–437.
14. Arispe, N., E. Rojas, and H. B. Pollard. 1993. Alzheimer disease amyloid β-protein forms calcium channels in bilayer membranes: blockade by tromethamine and aluminum. *Proc. Natl. Acad. Sci. USA*. 90:567–571.
15. Arispe, N., H. B. Pollard, and E. Rojas. 1994. The ability of amyloid β-protein [AβP(1–40)] to form Ca^{2+} channels provides a mechanism for neuronal death in Alzheimer's disease. *Ann. N. Y. Acad. Sci*. 747: 256–266.
16. Arispe, N., J. Diaz, and O. Simakova. 2007. Aβ ion channels. Prospects for treating Alzheimer's disease with Aβ channel blockers. *Biochim. Biophys. Acta*. 1768:1952–1965.
17. Kawahara, M., N. Arispe, Y. Kuroda, and E. Rojas. 1997. Alzheimer's disease amyloid β-protein forms Zn^{2+}-sensitive cation-selective channels across excited membrane patches from hypothalamic neurons. *Biophys. J*. 73:67–75.
18. Rhee, S. K., A. P. Quist, and R. Lal. 1998. Amyloid β-protein (1–42) forms calcium-permeable- Zn^{2+} sensitive channels. *J. Biol. Chem*. 273:13379–13382.
19. Zhu, L. H. Y. J., and R. Lal. 1999. Amyloid β-protein (1–40) forms calcium-permeable Zn^{2+} sensitive channels in reconstituted lipid vesicles. *Biochemistry*. 38:11189–11196.
20. Kourie, J. I., C. L. Henry, and P. Farrelly. 2001. Diversity of amyloid β protein fragment [1–40]-formed channels. *Cell. Mol. Neurobiol*. 3:255–284.
21. Kagan, B. L., Y. Hirakura, R. Azimov, R. Azimova, and M.-C. Lin. 2002. The channel hypothesis of Alzheimer's disease: current status. *Peptides*. 23:1311–1315.
22. Micelli, D., V. Meleleo, E. Picciarelli, and E. Gallucci. 2004. Effects of sterols on β-amyloid peptide (AβP 1–40) channel formation and their properties in planar lipid membranes. *Biophys. J*. 86:2231–2237.
23. Quist, A., I. Doudevski, H. Lin, R. Azimova, D. Ng, B. Frangione, B. Kagan, J. Ghiso, and R. Lal. 2005. Amyloid ion channels: a common structural link for protein-misfolding disease. *Proc. Natl. Acad. Sci. USA*. 102:10427–10432.
24. Lal, R., H. Lin, and A. P. Quist. 2007. Amyloid β ion channel: 3D structure and relevance to amyloid channel paradigm. *Biochim. Biophys. Acta*. 1768:1966–1975.
25. Durell, S. R., H. R. Guy, N. Arispe, E. Rojas, and H. B. Pollard. 1994. Theoretical models of the ion channel structure of amyloid-β-protein. *Biophys. J*. 67:2137–2145.
26. Jang, H., J. Zheng, and R. Nussinov. 2007. Models of β-amyloid ion channels in the membrane suggest that channel formation in the bilayer is a dynamic process. *Biophys. J*. 93:1938–1949.
27. Jang, H., J. Zheng, R. Lal, and R. Nussinov. 2008. New structures help the modeling of toxic amyloid β ion channels. *Trends Biochem. Sci*. 33:91–100.
28. Arispe, N., H. B. Pollard, and E. Rojas. 1996. Zn^{2+} interaction with Alzheimer amyloid β protein calcium channels. *Proc. Natl. Acad. Sci. USA*. 93:1710–1715.
29. Chakrabarti, P. 1990. Geometry of interaction of metal ions with histidine residues in protein structures. *Protein Eng*. 4:57–63.
30. Perlman, R. K., and M. R. Rosner. 1994. Identification of zinc ligands of the insulin-degrading enzyme. *J. Biol. Chem*. 269:33140–33145.
31. Becker, A. B., and R. A. Roth. 1993. Identification of glutamate-169 as the third zinc-binding residue in proteinase III, a member of the family of insulin-degrading enzymes. *Biochem. J*. 292:137–142.
32. Miura, T., K. Suzuki, N. Kohata, and H. Takeuchi. 2000. Metal binding modes of Alzheimer's amyloid β-peptide in insoluble aggregates and soluble complexes. *Biochemistry*. 39:7024–7031.
33. Yang, D. S., J. McLaurin, K. Qin, D. Westaway, and P. E. Fraser. 2000. Examining the zinc binding site of the amyloid-β peptide. *Eur. J. Biochem*. 267:6692–6698.
34. Mukherjee, A., and B. Bagchi. 2006. Anomalous orientation-dependent effective pair interaction among histidine and other amino acid residues in metalloproteins: breakdown of the hydropathy scale index. *Biochemistry*. 45:5129–5139.
35. Arispe, N. J. 2004. Architecture of the Alzheimer's AβP ion channel. *J. Membr. Biol*. 197:33–48.
36. Diaz, J. C., J. Linnehan, H. Pollard, and N. Arispe. 2006. Histidines 13 and 14 in the Aβ sequence are targets for inhibition of Alzheimer's disease Aβ ion channel and cytotoxicity. *Biol. Res*. 39:447–460.
37. Tickler, A. K., D. G. Smith, G. D. Ciccotosto, D. J. Tew, C. C. Curtain, D. Carrington, C. L. Masters, A. I. Bush, R. A. Cherny, R. Cappai, J. D. Wade, and K. J. Barnham. 2005. Methylation of the imidazole side chains of the Alzheimer disease amyloid-β peptide results in abolition of superoxide dismutase-like structures and inhibition of neurotoxicity. *J. Biol. Chem*. 280:13355–13363.
38. Bhattacharyya, R., R. P. Saha, U. Samanta, and P. Chakrabarti. 2003. Geometry of interaction of the histidine ring and other planar basic residues. *J. Proteome Res*. 2:255–263.
39. Scheiner, S., T. Kar, and J. Pattanayak. 2002. Comparison of various types of hydrogen bonds involving aromatic amino acids. *J. Am. Chem. Soc*. 124:13257–13264.
40. Saha, R. P., R. P. Bahadur, and P. Chakrabarti. 2005. Interresidue contacts in proteins and protein-protein interfaces and their use in characterizing the homodimeric interface. *J. Proteome Res*. 4:1600–1609.
41. Chakrabarti, P., and R. Bhattacharyya. 2007. Geometry of nonbonded interactions involving planar groups in proteins. *Prog. Biophys. Mol. Biol*. 95:83–137.
42. Gilman, A. G., T. W. Rall, A. S. Miles, and P. Taylor. 1993. The Pharmacological Basis of Therapeutics, 8th ed. McGraw Hill, New York.
43. Loo, D. T., A. Copani, C. J. Pike, R. E. Whittemore, A. J. Walencewicz, and C. W. Cotman. 1993. Apoptosis is induced by β-amyloid in cultured central nervous system neurons. *Proc. Natl. Acad. Sci. USA*. 90:7951–7955.
44. Lashuel, H. A., D. Hartley, B. M. Petre, T. Wall, and P. T. Lansbury Jr. 2002. Neurodegenerative disease: amyloid pores from pathogenic mutations. *Nature*. 418:291.